Discontinuous Maxwell-Rankine stress functions for space frames and plane grillages

Allan McRobie* and Chris Williams**

*Cambridge University Engineering Department
Trumpington St, Cambridge, CB2 1PZ, UK. fam20@cam.ac.uk
**Dept of Architecture and Civil Engineering, University of Bath,
Claverton Down, Bath BA2 7AY, UK. c.j.k.williams@bath.ac.uk

August 16, 2016

Abstract

This paper shows how bending and torsional moments in 3D frames can be represented via a discontinuous Maxwell-Rankine stress function. The Rankine reciprocal consists of polygons whose areas represent forces, but these need not be orthogonal to the beams. One consequence is a simple method for 2D grillage analysis via graphic statics.

Keywords: Maxwell stress function, Rankine reciprocal diagrams, graphic statics, grillage analysis, frames.

1 Introduction

Williams and McRobie [1] generalised Maxwell's reciprocal diagrams and graphical statics for 2D trusses to analyse the bending moments in 2D frames. The innovation was to consider an Airy stress function which possesses discontinuities. This paper applies similar ideas to the Maxwell-Rankine stress function to create a method applicable to 3D frames. Although the method becomes somewhat complicated and is currently incomplete, one consequence is that it reveals a simple graphical method for the analysis of 2D grillages.

For 2D trusses, Maxwell 1864 and 1870 presented a conceptual framework for the graphical representation of the forces in 2D pin-jointed trusses encompassing both form and forces via a pair of reciprocal diagrams. The diagrams were related via a polyhedral Airy stress function, where the change in slope at the boundary between any two adjacent faces of the polyhedron corresponds to the axial force in the member at that boundary. This was generalised in Williams and McRobie [1] to be applicable to 2D frames. Moments were then represented as discontinuities in the Airy stress function.

We now endeavour to extend these ideas to 3D. Maxwell 1870 presented two methods for applying a stress function approach in 3D. One of these, which we shall call the Maxwell-Rankine stress function, is a single scalar stress function. This leads to Rankine 3D reciprocals, with lines in one diagram being dual to areas in the other. The lines of the form diagram are the bars, and the axial forces in the bars are given by the area of the polygons in the reciprocal diagram which

are orthogonal to the bars. The underlying duality is that of 4D projective geometry, with (nodes, lines, polygons, cells) of one diagram being dual to (cells, polygons, lines, nodes) of the other.

Maxwell's other approach used three separate stress functions, and a triplet of reciprocal diagram pairs. We shall call these the Maxwell-Cremona stress functions, and these correspond to the Cremona duality in 3D, with line-like bars in one diagram parallel to line-like forces in the other. The underlying duality is that of 3D projective geometry, with (nodes, lines, polygons) of one diagram being dual to (polygons, lines, nodes) of the other.

In this paper we consider only the Maxwell-Rankine stress function. This appears to be the more natural 3D generalisation of the 2D Airy stress function approach. However, it is known that the Maxwell-Rankine stress function is incomplete, in that there exist equilibrium states of stress in 3D which cannot be represented by such a stress function. The only complete 3D stress function is the Beltrami stress function, but we do not consider that in any detail here.

In the 2D case, the units of the Airy stress function are [kNm], thus discontinuities in stress function have the units of bending moment. For the 3D Rankine case, the stress function has units of $\sqrt{\text{kN}}\text{m}$. This has gradient $\sqrt{\text{kN}}$, thus we can see that a product of a stress function discontinuity and a change of gradient gives the correct units of [kNm]. The proof that a meaningful bending moment can be modelled in this manner is the first main result in the paper.

As is demonstrated in McRobie [2], the 3D Maxwell-Rankine stress function can be most readily visualised by looking along any bar of interest. In that case the problem is reduced to a 2D stress function problem. The Maxwell-Rankine stress function restricted to a plane perpendicular to the bar resembles an Airy stress function, but its use is different. McRobie [2] refers to this restricted function as a "Mairy stress function". For a Mairy stress function, the stresses are perpendicular to - rather than in - the plane. Moreover, these normal stresses are given by the Gaussian curvature of the Mairy stress function (whereas in-plane stresses are given by second derivatives of the Airy stress function).

In the Airy stress function approach to 2D trusses, in-plane bar forces correspond to the change in slope across ridge lines of the polyhedral stress function. In this new 2D-slice-through-3D perspective, the Mairy stress function is again polyhedral, but the force is perpendicular to the plane and its magnitude is equal to the discrete Gaussian curvature at a node of the polyhedron. Simple ridges generate no force since their Gaussian curvature is zero. However, where a set of ridges meet at a node (which is actually the bar we are looking along) there can be a force perpendicular to the plane. For 3D trusses, the magnitude of that force is given by the area of the Gauss map in that vicinity, the Gauss map being a delineation of the Rankine polygon perpendicular to the bar. The Gaussian curvature (and thus the force) is also equal to the angular deficit at the node, but this is a less useful perspective.

The foregoing description applies only to axial forces in bars. In this paper we take the first steps to extending this to allow bars to carry bending moments in 3D. We should state from the outset that the resulting 3D version is far less visually intuitive than the 2D version of Williams and McRobie. Moreover, the method can presently only be applied to some rather simple cases.

1.1 Literature

The three classic papers are Maxwell [3, 4] and Rankine [5] which develop the ideas of reciprocal diagrams in 2D and 3D trusses, and which define the stress function considered here. This paper builds upon the formalism developed in Mitchell *et al.* [6], McRobie *et al.* [7], McRobie [2, 8], and is a generalisation of the idea put forward for 2D frames in Williams and McRobie [1]. Other recent work with stress functions and reciprocal diagrams for 3D trusses includes Akbarzadeh *et al.* [9, 10, 11] and Micheletti [12].

2 The Maxwell-Rankine stress function

Maxwell 1870 [4] defines two different stress function approaches to 3D stresses. One approach, which we call the Maxwell-Rankine stress function Φ, defines by the stresses to be a non-linear function of the stress function, via the following equations:

$$\sigma_{xx} = \frac{\partial^2\Phi}{\partial y^2}\frac{\partial^2\Phi}{\partial z^2} - \left(\frac{\partial^2\Phi}{\partial y \partial z}\right)^2 \quad (1)$$

$$\sigma_{yy} = \frac{\partial^2\Phi}{\partial z^2}\frac{\partial^2\Phi}{\partial x^2} - \left(\frac{\partial^2\Phi}{\partial z \partial x}\right)^2 \quad (2)$$

$$\sigma_{zz} = \frac{\partial^2\Phi}{\partial x^2}\frac{\partial^2\Phi}{\partial y^2} - \left(\frac{\partial^2\Phi}{\partial x \partial y}\right)^2 \quad (3)$$

$$\sigma_{yz} = \frac{\partial^2\Phi}{\partial z \partial x}\frac{\partial^2\Phi}{\partial x \partial y} - \frac{\partial^2\Phi}{\partial x^2}\frac{\partial^2\Phi}{\partial y \partial z} \quad (4)$$

$$\sigma_{zx} = \frac{\partial^2\Phi}{\partial x \partial y}\frac{\partial^2\Phi}{\partial y \partial z} - \frac{\partial^2\Phi}{\partial y^2}\frac{\partial^2\Phi}{\partial z \partial x} \quad (5)$$

$$\sigma_{xy} = \frac{\partial^2\Phi}{\partial y \partial z}\frac{\partial^2\Phi}{\partial z \partial x} - \frac{\partial^2\Phi}{\partial z^2}\frac{\partial^2\Phi}{\partial x \partial y} \quad (6)$$

which, in the absence of body forces, can readily be shown to satisfy the equilibrium equations

$$\frac{\partial\sigma_{xx}}{\partial x} + \frac{\partial\sigma_{xy}}{\partial y} + \frac{\partial\sigma_{xz}}{\partial z} = 0 \quad (7)$$

$$\frac{\partial\sigma_{yx}}{\partial x} + \frac{\partial\sigma_{yy}}{\partial y} + \frac{\partial\sigma_{yz}}{\partial z} = 0 \quad (8)$$

$$\frac{\partial\sigma_{zx}}{\partial x} + \frac{\partial\sigma_{zy}}{\partial y} + \frac{\partial\sigma_{zz}}{\partial z} = 0 \quad (9)$$

Any state of stress in 3D can be represented by a Beltrami stress function Ψ, this being a 3×3 symmetric tensor with 6 independent components, stresses being defined via

$$\sigma^{ij} = \epsilon^{ikm}\epsilon^{jln}\Psi_{kl,mn} \quad (10)$$

where ϵ is the Levi-Civita pseudotensor.

The Maxwell-Rankine stress function Φ is the Beltrami stress function Ψ with components

$$\Psi_{ij} = \Phi_{,i}\Phi_{,j} \quad (11)$$

Unlike the Maxwell-Rankine stress function, stresses are a linear function of the Beltrami stress function, and thus Beltrami stress functions can be linearly superposed.

Restricting attention to the Maxwell-Rankine case, it can be seen from the definition (Eqns. 1-6) that the stress tensor $\boldsymbol{\sigma}$ is simply the matrix of cofactors of the matrix of second derivatives (the Hessian) of the Maxwell-Rankine stress function. It is also apparent from Eqn. 1 that the stress σ_{xx} normal to a plane of constant $x = c$ is the Gaussian curvature of the stress function $\phi(y, z) = \Phi(c, y, z)$ on that plane. We shall call such a 2D stress function $\phi(y, z) = \Phi(c, y, z)$ (i.e. a restriction of the Maxwell-Rankine stress function to a given plane $x = c$) the "Mairy stress function" for that plane. The following constructions make much use of the Gaussian curvature of Mairy stress functions.

3 A simple proof for 3D bending

Consider a line-like bar which is a member of a 3D frame, and take the z coordinate to be along the bar (see Fig. 1a). At any point on the bar, the x and y axes divide the plane orthogonal to the bar into four quadrants. Let these quadrants be separated by thin regions around the axes (Fig. 1b). We choose a Maxwell-Rankine stress function $\Phi(x, y, z)$ which is independent of z. The Mairy stress function $\phi(x, y)$ is thus the same on all planes of constant z. Let the Mairy stress function decompose as $\phi(x, y) = f(x) + h(y)$ and let the function $f(x)$ consist of two linear regions, one of zero slope and one of slope g. The two regions are joined smoothly over the thin central region by a smoothly curved function. Also, let the function $h(y)$ consist of two flat plateaux which differ by a height Δ, joined by a smoothly curved transition over the thin region between them. The Mairy stress function and its first derivatives are thus continuous everywhere.

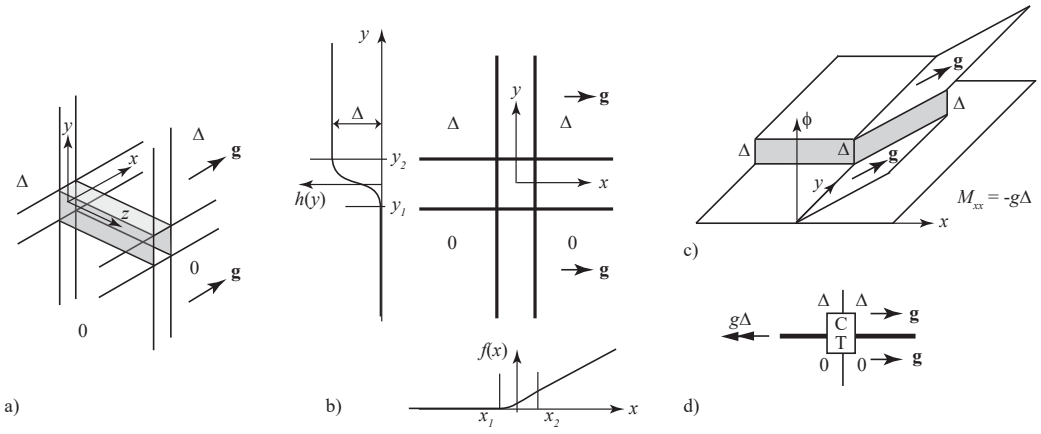

Figure 1: a) The bar in 3D space. b) A plane perpendicular to the bar, showing the Mairy stress function components $f(x)$ and $h(y)$. c) The Mairy stress function, as the size of the bar shrinks to zero. d) A diagrammatic representation of the resulting bending moment.

The matrix of second derivatives of the stress function is

$$\begin{pmatrix} \Phi_{,xx} & \Phi_{,xy} & \Phi_{,xz} \\ \Phi_{,yx} & \Phi_{,yy} & \Phi_{,yz} \\ \Phi_{,zx} & \Phi_{,zy} & \Phi_{,zz} \end{pmatrix} = \begin{pmatrix} f_{,xx} & 0 & 0 \\ 0 & h_{,yy} & 0 \\ 0 & 0 & 0 \end{pmatrix} \tag{12}$$

and the stresses are the cofactors of this. All stresses are thus zero except $\sigma_{zz} = f_{,xx} h_{,yy}$, and this is only non-zero over the small central rectangular region.

We obtain the axial force in the bar as

$$\begin{aligned} P_z &= \int_A \sigma_{zz}\, dx\, dy = \int_{x_1}^{x_2} f_{,xx}\, dx \int_{y_1}^{y_2} h_{,yy}\, dy \\ &= (f_{,x}|_{x_2} - f_{,x}|_{x_1})\,(h_{,y}|_{y_2} - h_{,y}|_{y_1}) = 0 \end{aligned} \tag{13}$$

since the slopes $h_{,y}$ transverse to the upper and lower boundaries are zero. It follows similarly that the moment M_{yy} about the y axis is also zero.

The moment about the x-axis is given by

$$\begin{aligned} M_{xx} &= \int_A y\sigma_{zz}\, dx\, dy = \int_{x_1}^{x_2} f_{,xx}\, dx \int_{y_1}^{y_2} y\, h_{,yy}\, dy \\ &= (f_{,x}|_{x_2} - f_{,x}|_{x_1}) \{[yh_{,y}]_{y_1}^{y_2} - \int_{y_1}^{y_2} h_{,y}\, dy\} \\ &= -(f_{,x}|_{x_2} - f_{,x}|_{x_1})(h(y_2) - h(y_1)) \qquad (14) \\ &= -g\Delta \qquad (15) \end{aligned}$$

This is a key result. The magnitude of the bending moment is the product of the change in slope g with the step height Δ. This results holds as the thicknesses of the thin dividing regions tend to zero.

As stated earlier, the Maxwell-Rankine stress function has units of $\sqrt{\text{kN}}$m, such that the product $g\Delta$ has units of $\left[\sqrt{\text{kN}}\right]\left[\sqrt{\text{kN}}\text{m}\right] = [\text{kNm}]$, the units of bending moment.

3.1 A simpler proof

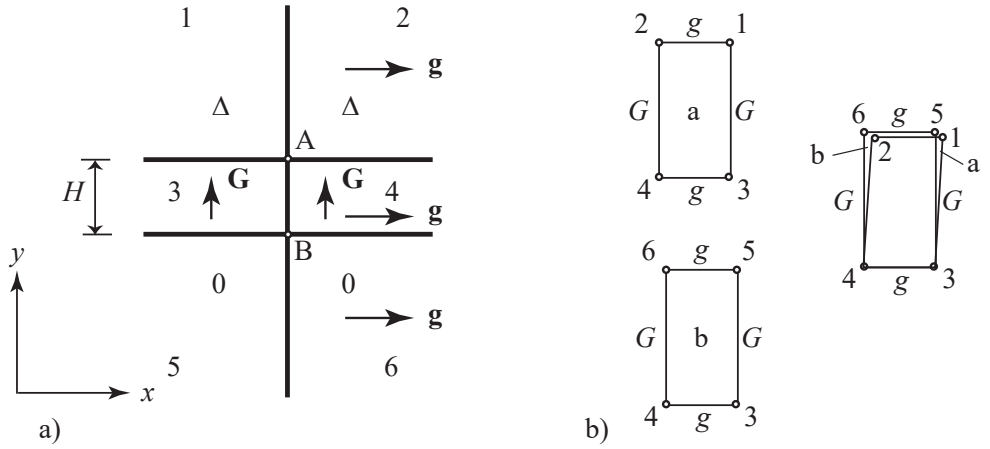

Figure 2: a) The Mairy stress function on the plane perpendicular to two parallel bars A and B. b) The Rankine polygons a and b reciprocal to the bars A and B.

Consider two parallel bars separated by a distance H carrying equal and opposite tension and compression forces. A polyhedral Mairy stress function over a plane perpendicular to both bars is shown in Fig. 2a. The stress function is linear over all six regions. Over the thin regions 3 and 4 of thickness H, the stress function rises sharply with gradient $\boldsymbol{G}$ to a height Δ. The (X, Y, Z) coordinates of the points reciprocal to each of the numbered cells are given by the negative of the gradients across that cell. For example, the point reciprocal to cell 4 has coordinates $(-g, -G, 0)$. The Rankine reciprocals of bars A and B are thus rectangles **a** and **b** each of area gG. These are oriented areas, and since they adjoin along the edge connecting reciprocal nodes 3 and 4, it follows that one area is positive and the other negative. The total axial force is thus zero. The moment about the x axis has magnitude $(gG)H$, but $GH = \Delta$, whence the moment has magnitude $g\Delta$. The sign convention for Mairy stress functions is that stresses are positive over elliptic regions and

negative over hyperbolic regions, thus B is in tension and A is in compression. This all agrees with our earlier proof.

4 Biaxial bending

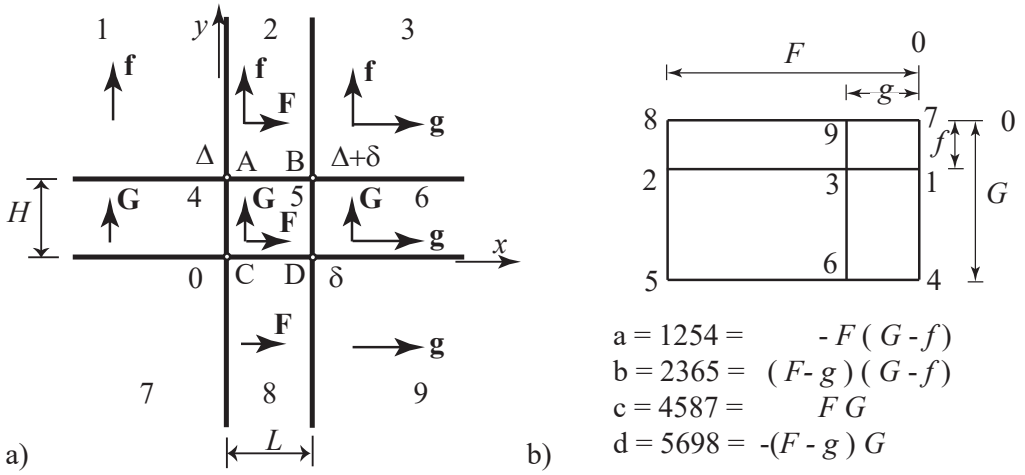

Figure 3: Biaxial bending. a) The Mairy stress function for bars A,B,C,D. b) The Rankine polygons reciprocal to bars A,B,C,D.

We adopt the simpler approach for the derivations here. Consider four parallel bars aligned along the z direction, and separated by distances H and L in a rectangular arrangement. Let the Maxwell-Rankine stress function have no variation with z and let there be a polyhedral Mairy stress function as shown in Fig. 3a. There are two overlapping narrow regions over which the stress function rises with steep slopes $\boldsymbol{F}$ and $\boldsymbol{G}$ to heights δ and Δ respectively. Beyond these are gentler slopes $\boldsymbol{g}$ and $\boldsymbol{f}$ respectively.

Reciprocal to each bar is a rectangle, as shown in Fig. 3b. The stress function around bars B and C is locally elliptic, thus these are in tension. The oriented areas of each rectangle are given in Fig. 3b. Summing these shows that the total axial force is fg. The moment about the x-axis (with origin at C) is given by $(a+b)H = (-gG+gf)H$, and about the y-axis is $(b+d)L = (-fF+gf)L$. Letting H and L shrink, such that slopes $F = \delta/L$ and $G = \Delta/H$ become large compared to f and g, we obtain the moments $-g\Delta$ and $-f\delta$ about the x- and y-axes respectively. Again each is the product of a step change in the stress function with the slope change along that step.

This example generates a specific coexistent axial force gf. To create a bar with any desired axial force and biaxial moments, the values of g, f, δ and Δ may be chosen accordingly. If these are pre-defined by conditions elsewhere, the axial force can be varied separately via further subdivision of the stress function, in the manner shown in Fig. 4. There, cell 3 has been split into two cells. By varying this subdivision, the axial force - given by the area of the reciprocal pentagon - can be varied without changing the moments $g\Delta$ and $f\delta$. It is clear that one possibility is a bar of zero oriented area, corresponding to no axial force.

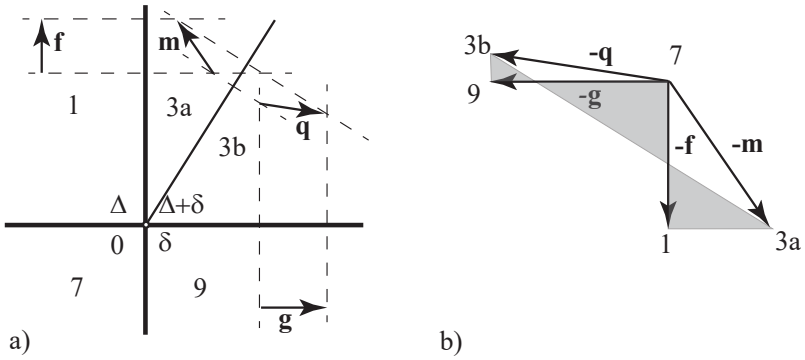

Figure 4: a) A Mairy stress function where the axial force may be adjusted separately from the biaxial bending. b) The Rankine polygon reciprocal to the bar.

5 Torsion

Figure 5 shows a bar and an associated Maxwell-Rankine stress function. There is a smooth step of Δ as one across the x axis, and a smooth step of gz as one moves across the y axis. The stress function is $\Phi = gzf(x) + \Delta h(y)$. The functions $f(x)$ and $h(y)$ are smoothed unit step functions. The matrix of second derivatives of the stress function is

$$\begin{pmatrix} \Phi_{,xx} & \Phi_{,xy} & \Phi_{,xz} \\ \Phi_{,yx} & \Phi_{,yy} & \Phi_{,yz} \\ \Phi_{,zx} & \Phi_{,zy} & \Phi_{,zz} \end{pmatrix} = \begin{pmatrix} gzf_{,xx} & 0 & gf_{,x} \\ 0 & \Delta h_{,yy} & 0 \\ gf_{,x} & 0 & 0 \end{pmatrix} \tag{16}$$

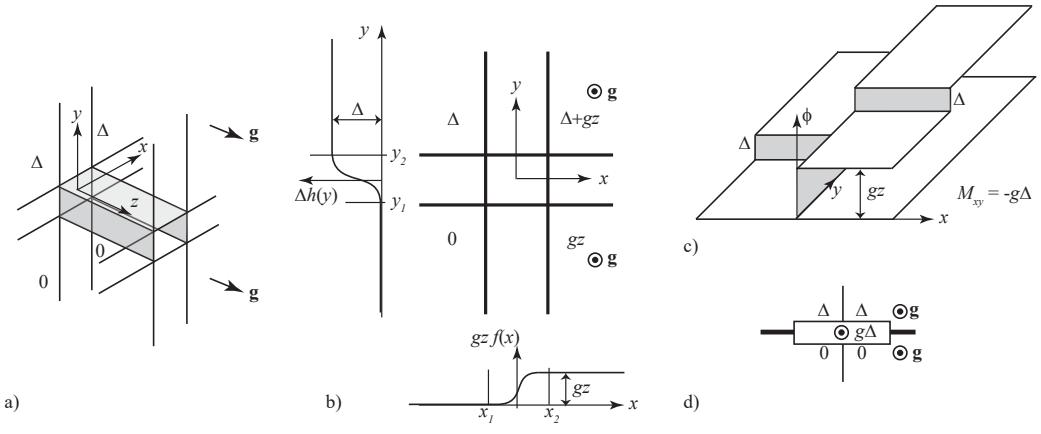

Figure 5: a) The Maxwell-Rankine stress function around a bar in pure torsion b) The Mairy stress function on a plane perpendicular to the bar is the sum $\Phi = gzf(x) + \Delta h(y)$ where $f(x)$ and $h(y)$ are smoothed unit step functions. c) The Mairy stress function in the limit as the thickness of the separating layers tends to zero. d) A simple diagrammatic representation.

The stresses are given by the matrix of cofactors

$$\boldsymbol{\sigma} = \begin{pmatrix} 0 & 0 & -gf_{,x}\Delta h_{,yy} \\ 0 & -g^2 f_{,x}^2 & 0 \\ -gf_{,x}\Delta h_{,yy} & 0 & -gzf_{,xx}\Delta h_{,yy} \end{pmatrix} \tag{17}$$

These are zero everywhere except over the central bar region. There, we obtain the axial force

$$\begin{aligned} P_z &= \int_A \sigma_{zz}\, dx\, dy = gz \int_{x_1}^{x_2} f_{,xx}\, dx\, \Delta \int_{y_1}^{y_2} h_{,yy}\, dy \\ &= gz\,[f_{,x}]_{x_1}^{x_2}\,\Delta\,[h_{,y}]_{y_1}^{y_2} = 0 \end{aligned} \tag{18}$$

This follows because the slope $f_{,x}$ is zero at x_1 and x_2, and $h_{,y}$ is zero at y_1 and y_2. These also imply the bending moments are zero, since

$$M_{xx} = \int_A y\sigma_{zz}\, dx\, dy = gz\,[f_{,x}]_{x_1}^{x_2}\,\Delta \int_{y_1}^{y_2} yh_{,yy}\, dy = 0 \tag{19}$$

$$M_{yy} = \int_A x\sigma_{zz}\, dx\, dy = gz \int_{x_1}^{x_2} xf_{,xx}\, dx\, \Delta\,[h_{,y}]_{y_1}^{y_2} = 0 \tag{20}$$

The torsion, however, is given by

$$\begin{aligned} T = M_{xy} &= \int_A y\sigma_{zx}\, dx\, dy = -g \int_{x_1}^{x_2} f_{,x}\, dx\, \Delta \int_{y_1}^{y_2} yh_{,yy}\, dy \\ &= -g\,[f]_{x_1}^{x_2}\,\Delta \left([yh_{,y}]_{y_1}^{y_2} - \int_{y_1}^{y_2} h_{,y}\, dy \right) \\ &= g\,[1]\,\Delta\,[h(y_2) - h(y_1)] = g\Delta \end{aligned} \tag{21}$$

This is the second main result of this paper: the torsion in a bar is the product of the step discontinuity Δ across the bar in one direction (y, say) with the change in slope g parallel to the bar as one crosses the bar in the other (x) direction.

6 Special Case 1: 2D frames

Having developed a theory for individual beams in 3D, we now begin to connect them together to make frames. We begin with simple special cases, the first of which is 2D frame action. The frame will lie in the horizontal $z = 0$ plane. The z-variation of the Maxwell-Rankine stress function will be a slope discontinuity of G across the $z = 0$ plane, as illustrated in Fig. 6. We consider the case where two bars meet at a right angle joint. For all z, the x, y variation consists of a step of Δ in the positive x, y quadrant, within the corner of the joint.

Cross-sections perpendicular to each beam reveal the diagrammatic representations from Fig. 1, from which we conclude that each beam carries a bending moment about the z axis of magnitude $G\Delta$.

Fig. 7 shows the corresponding 3D representation for a beam carrying an axial force. Again the only z-variation of the stress function has a slope change of G on crossing the $z = 0$ plane. If the beam x-direction is chosen to be along the beam, the x, y variation of the stress function is a slope change of g on crossing the $y = 0$ plane.

The beam forms the boundary of four rectilinear cells, and the coordinates of its Rankine reciprocal polygon are given by the negative of the gradients of the cells. This gives a rectangle, of area Gg, this being the axial force in the beam.

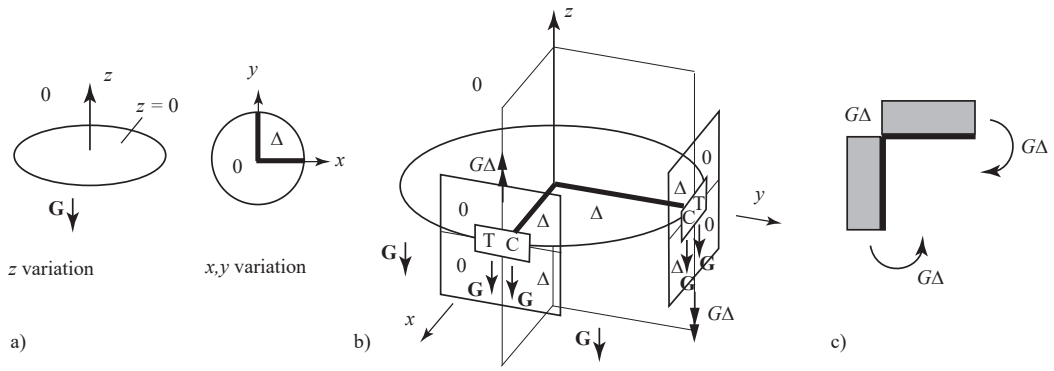

Figure 6: a) The z and the x, y variations of the Maxwell-Rankine stress function for two beams meeting at a right angled corner. b) A 3D representation of the full stress function, showing cross-sections perpendicular to the beams. c) The resulting bending moment diagram, as represented traditionally.

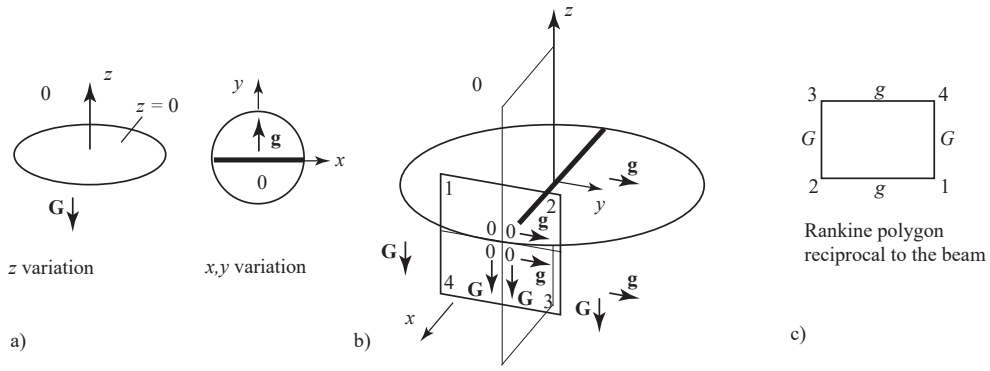

Figure 7: a) The z and the x, y variations of the Maxwell-Rankine stress function for a beam carrying an axial force. b) A 3D representation of the full stress function, showing a cross-section perpendicular to the beam. c) The Rankine polygon reciprocal to the beam.

The 3D Maxwell-Rankine stress function for 2D frame analysis is $\Phi(x, y, z) = Gh(z) + \phi(x, y)$, where $h(z)$ is the piecewise linear function that has unit slope change at $z = 0$, and $\phi(x, y)$ is the (possibly discontinuous) Airy stress function for the truss or frame. The units of the Airy stress function, in this case, are $\sqrt{\text{kNm}}$ (to match those of the Maxwell-Rankine stress function). The change of z-slope, G, is then a constant factor in all calculated quantities, with moments being $G\Delta$ and axial forces Gg. (Again, shear forces are given by the change in parallel slope as one crosses the beam.) Rather nicely then, we have distilled the whole of traditional graphic statics (and its extension by Williams and McRobie [1] via discontinuous Airy stress functions) from the full 3D Maxwell-Rankine theory.

Fig. 8 shows the simplest example - the triangular truss (Figure 1 of Maxwell 1864 [3]). Bar forces are given by areas of rectangles in the Rankine reciprocal. However, since all such rectangles have depth G, the bar forces are proportional to the horizontal edge lengths in the reciprocal diagram, as per standard 2D Maxwell reciprocals.

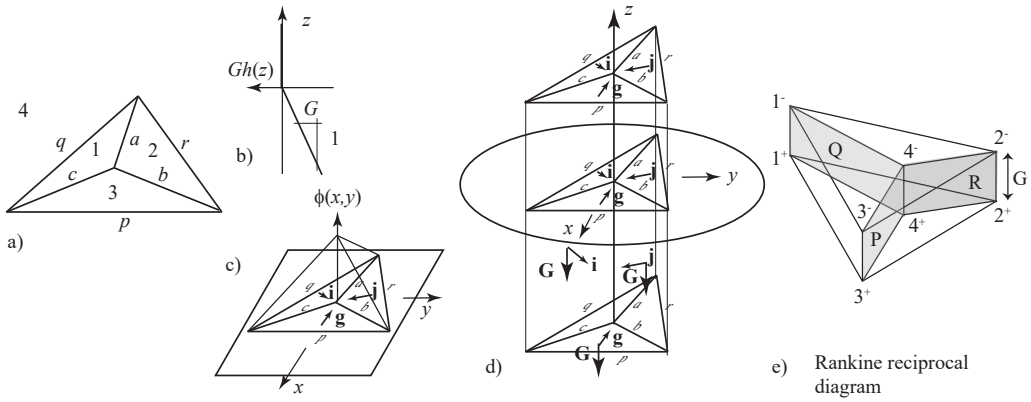

Figure 8: a) The simple triangular truss of Fig. 1 of Maxwell 1864. b) The z and the x, y variations of the Maxwell-Rankine stress function. c) A 3D representation of the full stress function, showing 8 cells. d) The Rankine reciprocal, with 8 nodes. Bar forces are given by rectangular areas orthogonal to the original bars.

6.1 Technicality: transverse stresses

There is a technicality that arises in the way that a Maxwell-Rankine stress function of this form gives rise to stresses (and in some cases infinite stresses) perpendicular to the plane of the frame. Maxwell [4] refers to just such problems. The issue can be seen in Fig. 9. The cells of the Rankine reciprocal have horizontal polygons at the top and bottom, and the areas of these correspond to forces along the vertical edges of the original cells. The diagram illustrates that there is a tensile force in the bar n, of magnitude equal to the area of the reciprocal triangle N.

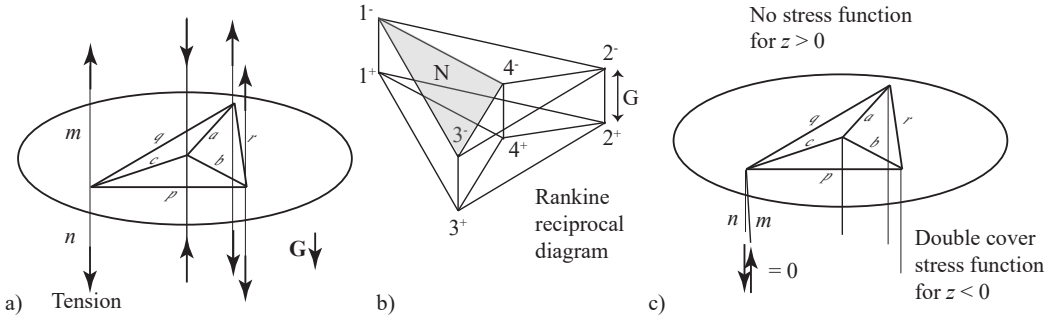

Figure 9: a) The Maxwell-Rankine stress function generates transverse forces orthogonal to the plane of the 2D truss. b) The magnitudes of these forces are given by the areas of the horizontal polygons that form the upper and lower faces of the Rankine reciprocal. c) By applying the stress function over a double cover of the negative z half-space, transverse forces are removed.

Although one could choose to simply ignore these transverse forces, a more elegant solution is to fold the stress function back over onto itself across the $z = 0$ plane. That is, the stress function is applied over a double cover of the lower z half-space. With this construction, all stresses perpendicular to the $z = 0$ plane have equal and opposite counterparts in the other half-space, and thus cancel. The tension N in n cancels with an equal and opposite compression M in the (folded

over) member m. Since these two members are now coincident in space in the double-half-space stress function construction, all transverse forces are thus removed, leaving only the in-plane forces of the 2D truss of interest.

Finally we note that, in 2D graphics statics, one may consider the area exterior to the structural perimeter to be the surface over which the Airy stress function acts, or one may consider the stress function to be double layered over the interior of the structural perimeter. This latter interpretation accords more neatly with the concept of the truss as the projection of a polyhedron, and - although points at infinity present few problems - it is neater to work within a finite conceptual framework. The double layer also presents advantages - often removing the need to insert additional nodes where bars cross, since the bars may be in different covers.

If one were to apply this idea to the 3D constructions illustrated here, then, for example, region 4 of Fig. 8a could be taken as the interior, rather than the exterior of the surrounding triangle pqr. If this is combined with the idea of folding the stress function through the $z = 0$ plane, one arrives at a quadruple cover of the prismatic region that extends below the truss diagram.

For the present, all such double and even quadruple covers are largely of academic interest, and it is easier to work with a single cover of the whole space. What is more important is to recognise that this section has demonstrated that standard 2D graphic statics and its Williams-McRobie extensions are naturally contained within the 3D conceptual framework being developed here. In the next section, we consider what else may be contained therein.

7 Special Case 2: Grillage analysis (no shear)

Another special case emerges from the 3D theory if the stress function is again partitioned into a z variation and an x, y variation. In this case we choose the only z variation to be a step of Δ as one crosses the $z = 0$ plane. The resulting stress function gives a model for the states of self-stress of a plane grillage, involving beam torsions and bending moments. In the first instance we consider the no-shear case - that is, the bending moments are constant along each beam.

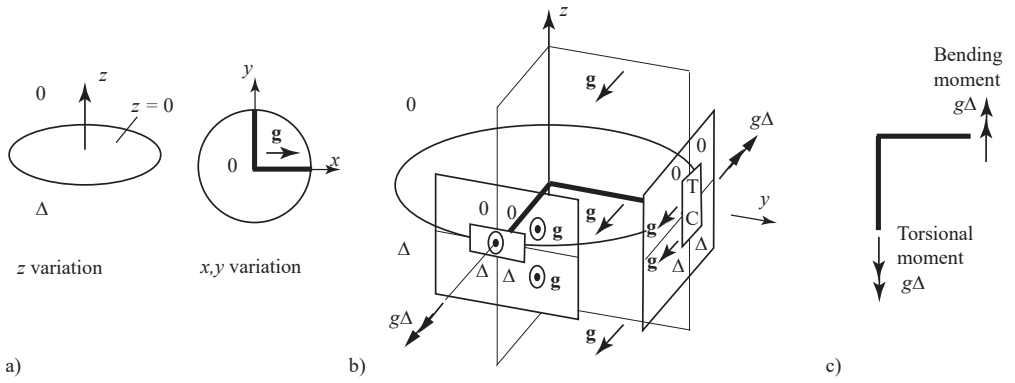

Figure 10: a) The z and x, y variations of the Maxwell-Rankine stress function to model two beams meeting in the manner of a grillage. b) The full Maxwell-Rankine stress function and the resulting bending and torsional moments. c) A traditional depiction of this situation.

To model two no-shear grillage bars meeting at a corner, we apply a stress function gx over the positive x, y quadrant, for all z. Fig. 10 illustrates the stress function, and the diagrammatic symbols on planes perpendicular to the beams. The morphology on the plane perpendicular to the y direction beam is the standard one for bending. The morphology on the plane perpendicular to

the beam in the x axis is that of torsion. This is a result of the stress function having a change g in the gradient parallel to the beam, as one crosses perpendicular to the beam on the x, y plane.

Fig. 10c shows the more traditional representation of this configuration, showing how the torsion in one beam is balanced by the bending moment in the other. We have thus successfully joined two beams around a corner, but in the fashion of a grillage.

This special case of the full 3D Maxwell-Rankine theory has thus led to a new 2D graphical method for 2D grillage analysis. It manifests itself on the $z = 0$ interface when there is a step of Δ across that interface. As when distilling 2D truss analysis from the fully 3D case, there will be stresses transverse to the plane. However, these will again be equal and opposite, and their effects can be removed by the device of the double-cover on the half-space below $z = 0$.

Whereas the previous section merely showed how the 3D theory agreed with known 2D methods, this section has arrived at a new 2D method. We thus temporarily drop the 3D methodology to briefly explore this new graphical method in 2D alone.

7.1 Graphic Grillage Analysis

For 2D truss and frame analysis, the fundamental object is the polyhedral Airy stress function, whose changes of slope and discontinuities in value lead to the forces and moments in the beams. For grillage analysis there is a similar stress function, but it does not yet appear to have a name. We therefore choose to call it the *grillage stress function*. Although derived from the Maxwell-Rankine stress function, for which the stresses are nonlinear functions of the stress function, the stress resultants are linear functions of the grillage stress function, and thus linear superposition can be applied.

As demonstrated in section 2, as one crosses a beam in the plane of the grillage, the change in the gradient perpendicular to the beam gives the bending moment in the beam, whilst the change in the gradient parallel to the beam gives the torsion. Discontinuities in value either side of a beam have no effect. A more general statement is to consider the combination of bending and torsional moments on a beam cross-section to be a general moment vector. The moment vector is then given by the difference in the gradient vectors of the grillage stress function either side of the beam.

Akin to 2D truss analysis, the underlying geometric framework for 2D graphic grillage analysis is 3D projective geometry. For each grillage diagram we can define a reciprocal grillage diagram. The duality is between (nodes, lines, faces) of one diagram and (faces, lines, nodes) of the other. For a polyhedral grillage stress function ϕ, the origin-based normals to each face can be intersected with the $\phi = 1$ plane to obtain the nodes reciprocal to those faces. It follows that the coordinates of a node j reciprocal to a face J are $-\boldsymbol{g}$, where $\boldsymbol{g}$ is the gradient of the grillage stress function over the original face J. A beam separating two original faces has, as its reciprocal, a line joining the two nodes reciprocal to those two faces. An original node which is the meeting point of n beams has as its reciprocal an n-sided polygon. This is simple equilibrium. Moment equilibrium requires the n moment vectors to add to zero (i.e. close the polygon). Note that, unlike in classical graphic statics for 2D trusses, reciprocal lines for grillage beams need no longer be orthogonal to their original duals.

7.2 Simple examples of graphic grillage analysis

Fig. 11a shows a rectangular grillage. We take the grillage stress function to be zero everywhere outside the frame, and to be a linear function with a gradient $\boldsymbol{g}$ parallel to two opposite edges. The stress function can be readily envisaged as akin to the glass in an opened skylight window, the window pivoting about a central axis (Fig. 11b). Clearly the transverse slope changes for two opposite beams while there is a change in the parallel slope for the other two beams. Two beams are thus in pure bending, connected by two beams in pure torsion. This is an admissible state of self-stress. Adding a constant to the stress function within the frame does not change the moments (Fig. 11b).

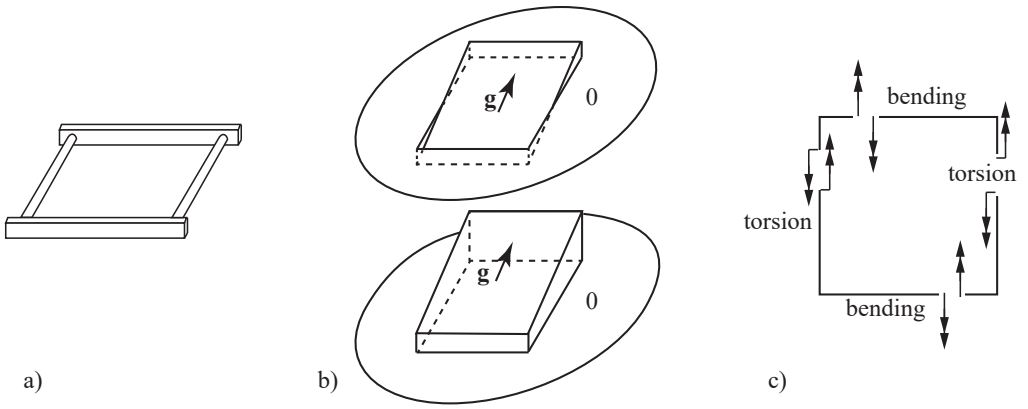

Figure 11: a) A simple rectangular grillage. b) Grillage stress functions which lead to the same bending and torsional moments. c) A traditional depiction of this situation.

Fig. 12a shows a circular ring subject to equal and opposite torques of magnitude $2g$ applied at points on a diameter. The general moment on any cross-section is simply $\boldsymbol{g}$, and this can be resolved into components of bending and torsion. The grillage stress function is the same as the Airy stress function of Williams and McRobie [1] for the case of in-plane bending of a circular beam under diametrically opposed point forces. The general equilibrium solution, including any state of grillage prestress, can be achieved by tilting the central disc in either direction.

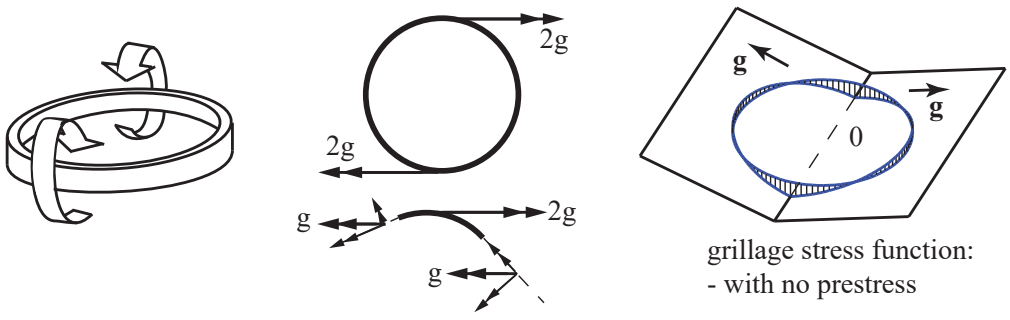

Figure 12: A circular ring subject to equal and opposite torques applied at diametrically opposite points.

Fig. 13a shows a triangular grillage (black). In plan, it is the same as the truss of Maxwell

1864, Fig 1. A general grillage stress function is shown in Fig. 13b. The coordinates of the nodes reciprocal to the original four plane regions are given by the negative of the gradients of the stress function. A beam that is the common edge of two adjacent plane regions in the original diagram has as its reciprocal a line connecting the two corresponding reciprocal nodes. This has been overlain in red on Fig. 13a. This strongly resembles the original diagram of Maxwell 1864, excepting that beams and their reciprocal lines need no longer be orthogonal. The grillage reciprocal is thus more general than for the 2D truss case.

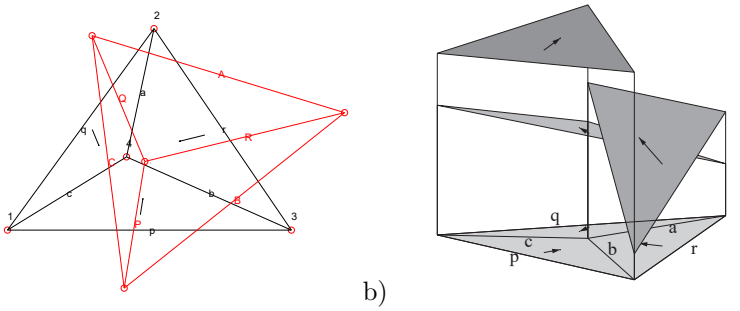

a) b)

Figure 13: a) In black is a plan of the triangular grillage having the same geometry as the 2D truss of Fig.1 of Maxwell 1864. b) A general grillage stress function over the grillage. The negatives of the gradients of the plane surfaces define the coordinates of the reciprocal diagram, shown in red in a). Note that beams and their reciprocal lines are no longer orthogonal.

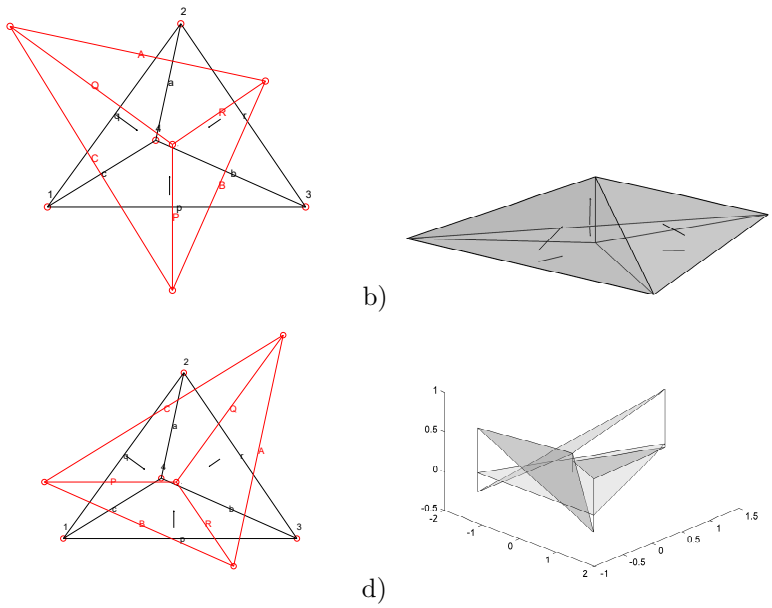

a) b)

c) d)

Figure 14: a) The form (black) and force (red) diagram for a pure-bending state of self stress of a triangular grillage. b) The corresponding grillage stress function, which is continuous. c) Form and force diagrams for a pure torsion state of self stress. d) The corresponding grillage stress function takes the gradients of the pure-bending stress function of (b) and rotates them by 90- degrees.

Fig. 14 shows a continuous grillage stress function over the triangular grillage. This grillage stress function is identical to the Airy stress function over Maxwell's original 2D truss. The continuity implies that the parallel components of the gradients either side of a beam are equal, and thus there is no torsion. The reciprocal diagram thus represents a state of self-stress where the grillage is in pure bending. As per the 2D truss, lines and their reciprocals are now perpendicular, and the reciprocal diagram for the pure-bending grillage is identical to Maxwell's 2D truss reciprocal.

If we now rotate the gradient vectors by 90 degrees (Fig. 14d), it follows that although there are now discontinuities in the grillage stress function, there is no change in transverse gradient across any beam. This corresponds to a state of grillage self-stress of pure torsion. Since torsion vectors are parallel to the beams, the resulting reciprocal diagram will be as for the 2D truss, but drawn in the Cremona (parallel) convention (Fig. 14c).

7.3 No-shear grillage-Minkowski diagrams

McRobie [8] put forward the concept of a Maxwell-Minkowski diagram which combines the form and force diagrams for a 2D truss into a single object. The same construction can be applied to the no-shear grillage form and force diagrams. The only difference is that because original and reciprocal bars are no longer orthogonal, the original and reciprocal diagrams are now connected together by parallelograms. An example is given for the case of the triangular grillage with a general state of grillage self-stress in Fig. 15.

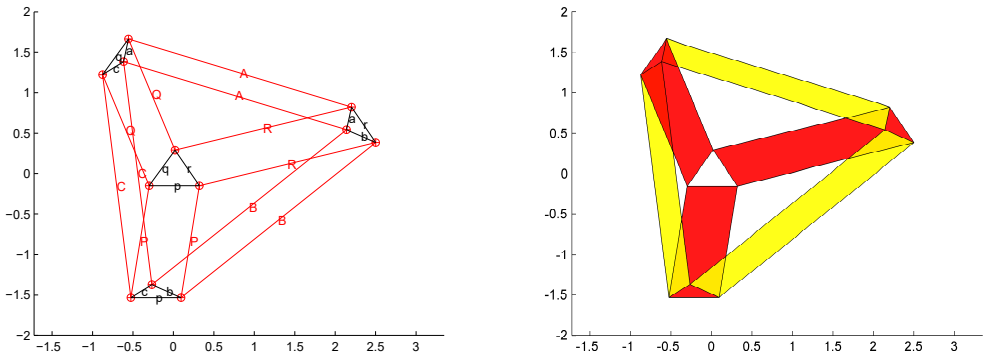

Figure 15: Grillage Minkowski diagrams for the triangular grillage of Fig. 13. Because beams and their reciprocals are no longer orthogonal, the original and reciprocal figures are connected by parallelograms.

For a pure-torsion grillage, the moment vector is parallel to the beam, and one obtains the extreme case where the parallelograms have zero width in one direction (Fig. 16).

7.4 Load Path Theorems for No-shear Grillages

One immediate consequence of the Minkowski construction is the implication that grillages possess two analogues of Maxwell's Load Path Theorem. Given that the Minkowski diagram gives a double cover of the overall region, and that each layer of the cover contains a copy of the form and force diagram, it follows that the total area of the red parallelograms in the Minkowski diagram of Fig. 15 must equal that of the yellow ones. Each parallelogram is an oriented area, and the fuller statement is that the total oriented area of all parallelograms is zero.

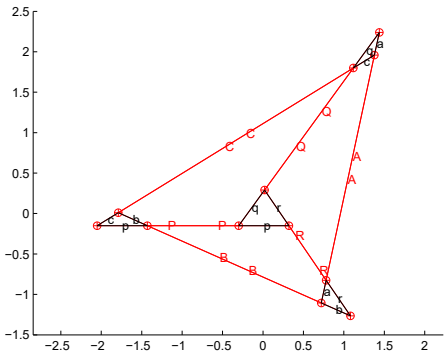

Figure 16: A grillage Minkowski diagram for the pure torsion solution of the triangular grillage of Fig. 14. Because beams and their reciprocals are parallel, the connecting parallelograms have zero width perpendicular to the beams.

Since the bending moment M is perpendicular to the bar, it follows that the area of the parallelogram is ML, thus

$$\sum ML = 0 \tag{22}$$

where M is the bending moment in the beam of length L. Currently, this proof only applies to no-shear grillages where the bending moment is constant along each beam.

Since a Minkowski diagram can be constructed from any original figure by combining it with any diagram which is topologically (rather than geometrically) equivalent to its reciprocal, it follows that an original can also be combined with a 90 degree rotation of its reciprocal. The area of parallelograms argument then implies that

$$\sum TL = 0 \tag{23}$$

where T is the torsion.

These two equations are analogues of the Maxwell Load Path Theorem for trusses, which has applications in structural optimisation (see e.g. Beghini *et al.* [13]).

7.5 Non-orthogonal reciprocals for 2D frames

The previous sections showed how reciprocal diagrams for 2D shear-free grillages could have reciprocal members which were not orthogonal to their original members. This arose because the moment at any section has two components - a torsional component along the beam and a bending component transverse to the beam, which together define a general moment vector which is not in general orthogonal to the beam. If we now revisit the Williams-McRobie [1] description of 2D frames, we see that a similar situation arose there, but has not yet been commented on. At each cross-section there is a general force consisting of an axial component and a shear component. Everything that has been said above about non-orthogonal reciprocal diagrams thus also applies to the 2D frame case. In the Maxwell convention for reciprocals, axial forces are drawn perpendicular to the original members, thus the shear forces will be parallel to the originals. Maxwell-Minkowski diagrams will thus involve joining the original and reciprocals together with parallelograms. In particular, it follows from the 90 degree rotation argument that there is a Load Path Theorem

$$\sum SL = 0 \tag{24}$$

for the in-plane shear forces in a 2D frame.

8 A space beam

In this section we take the first step towards a fully 3D theory, by placing the plane of a 2D moment frame orthogonal to the plane of a 2D grillage, and considering a bar that is common to both planes. The arrangement is shown in Fig. 17a. In the simplest case, we take the torsion in a bar a in the grillage, transfer it at a joint to the bending in the common bar b, and then take that bending around a corner in the 2D frame to the bar c.

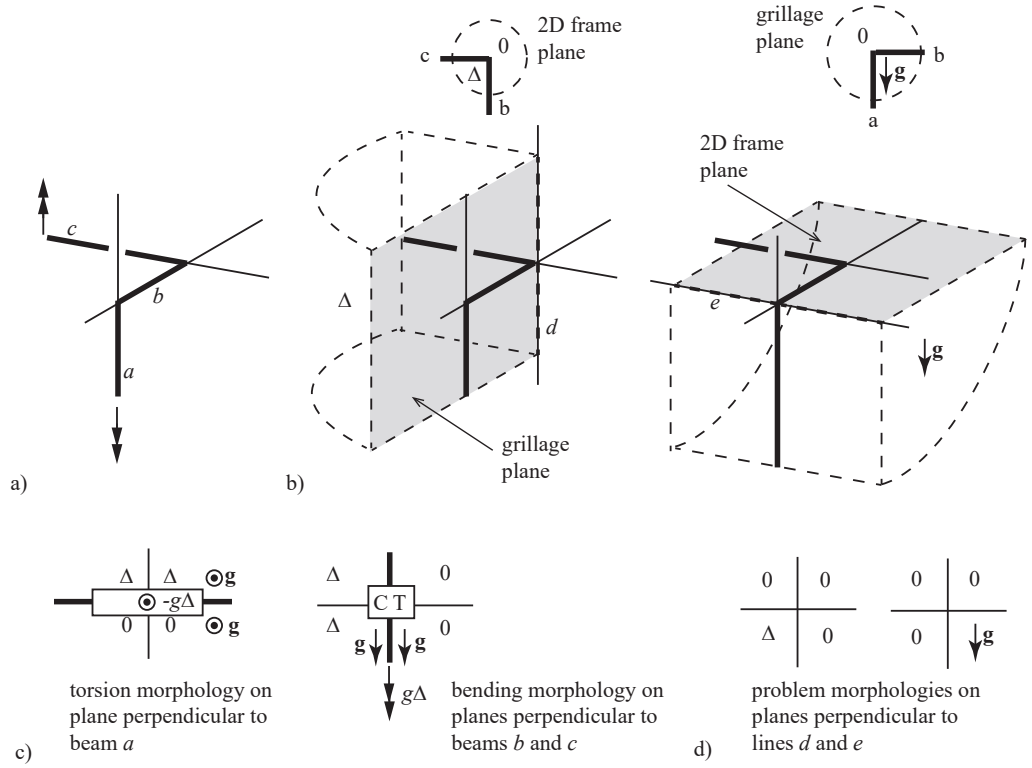

Figure 17: a) A space beam consisting of three segments. b) A Maxwell-Rankine stress function to transfer grillage torsion to 2D-frame bending. c) The stress function morphologies on sections perpendicular to the beams. d) Problematic stress function morphologies on sections perpendicular to lines d and e.

Bars in 2D frames and in grillages each involve a step change Δ and a slope change $\boldsymbol{g}$. One change occurs across the plane, and the other in the plane. By choosing a suitable Maxwell-Rankine stress function with a value Δ in one region, and a slope $\boldsymbol{g}$ in another (partially overlapping) region, the grillage-to-frame transfer can be accomplished along the various boundaries (Fig. 17b).

Taking sections perpendicular to the bars a, b and c shows that the stress function over each has the correct morphology (Fig. 17c). Taking sections normal to the non-bar extensions of the lines a, b and c reveals that no stresses are generated there. The difficulty arises with the lines d and e. Sections normal to these (Fig. 17d) reveal forces and moments along these lines. These

have no overall effect on the main beams, since each line is orthogonal to a bar joint, and the actions either side of the joint are in mutual equilibrium. These could even be effectively removed by simply folding the stress function over the two main planes, i.e. one fold over the grillage plane and one fold over the plane of the 2D frame. However, whilst this may work for this simple case, difficulties will be encountered in more general cases - for example, if lines d and e were intended to be unstressed beams.

9 Shear in grillage beams

Thus far, all bending moments in grillage beams have been constant along their length. We now consider how to include shear, such that bending moments can vary along their length. Since, for the grillage stress function, the bending moment is proportional to the transverse slope change across the beam, it would appear, at first sight, that letting this transverse slope change linearly along the length of the beam would thus give a linearly-varying bending moment. Taking the window frame example of Fig. 11, if the glass of the window frame were a hyperbolic surface of the form $\phi = xy$, (x, y being the plane of the grillage frame) then the transverse slopes would vary linearly around the edges. However, this does not give the correct solution.

Instead, recall that the bending moment in a grillage beam is given by the product $g\Delta$, where g is the change of transverse slope across the beam in the grillage plane, and Δ is the step change as we pass across the grillage plane. Changes in bending moment along a grillage beam can thus be accomplished by varying the step change Δ, rather than the transverse slope change g.

9.1 A simple example

Shear in beams is readily modelled in the 2D frame model of Williams and McRobie [1], and the previous space beam example has shown how it is possible to couple a grillage with a 2D frame by having orthogonal grillage and frame planes, with a beam common to both. The general idea of the next example, then, is to take the torsional moment out of a grillage frame, put it into a beam common to grillage and 2D frame planes, and once into the 2D frame plane, shear forces can be readily dealt with.

We consider the rectangular grillage of Fig. 11, but this time it is on supports near its corners, and we consider the case where the torsions in the two side bars are in the same (rather than opposite) directions. The connecting beams are thus each put into double curvature by equal (rather than equal and opposite) end moments. There is thus a shear in each of the beams, and to maintain moment equilibrium, there are support reactions. For clarity, we move the supports in from the corners a little.

The grillage stress function is still as per Fig. 11, resembling a partially opened window. However, rather than having a constant step Δ across the grillage plane, we let the step be a continuous piecewise-linear function, that varies from a plateau Δ to a plateau $-\Delta$ as we move from left to right. The change in slope occurs at the supports. This is then the 2D frame stress function.

The total Maxwell-Rankine stress function is then simply the sum of the grillage stress function and the 2D frame stress function. Fig. 18 shows the general idea, the torsions being taken from the grillage members to the cross-beams, where the shear is dealt with by the 2D frame stress function.

This is an interesting example as it is the first demonstration that transverse forces can be applied to a grillage. The idea of stitching together grillage and frame action in this manner is comparatively general, and a great many other interesting cases can be constructed by this method. The opportunities and the problems involved are a subject for further research.

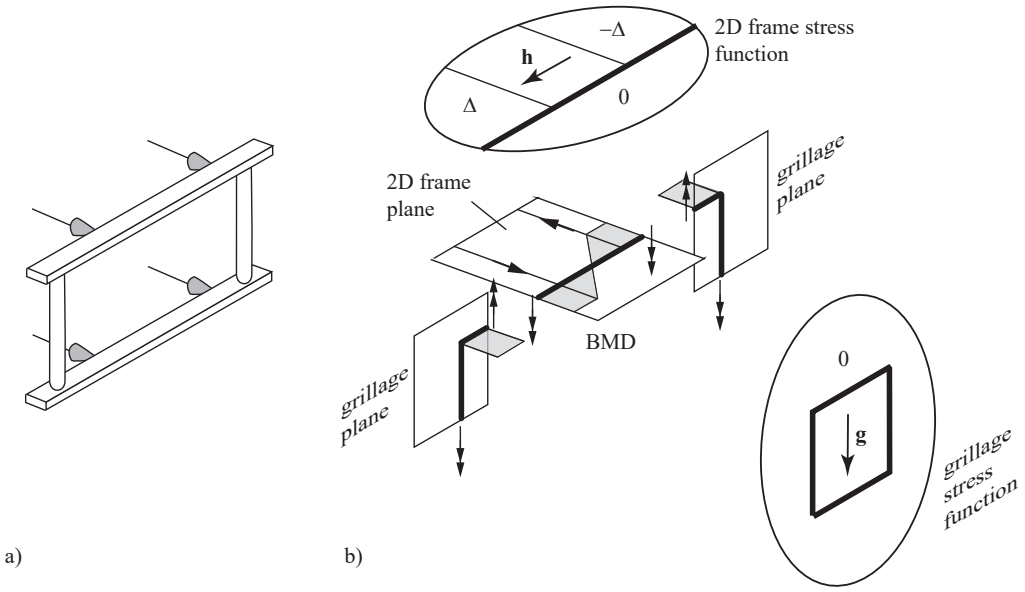

Figure 18: a) A grillage with support reactions. b) A Maxwell-Rankine stress function obtained by adding a grillage stress function to an orthogonal 2D frame stress function. Grillage torsion is transferred to 2D-frame bending, where applied forces and shears can be readily dealt with.

9.2 The Rankine reciprocal for grillages with shear

In the earlier examples of no-shear graphic grillage analysis, the 2D reciprocal diagrams represented the bending moment in a beam as a line perpendicular to the beam, the length being equal to the moment. If moment is now to vary along the beam, it would seem that this may present problems for any graphical representation. However, a graphical solution does exist for grillages with shear, and it requires us to return to the full 3D Rankine construction.

The fundamental concept, as ever, is to divide the form space into cells, and reciprocal to each cell is a point whose coordinates are given by the negative of the gradient of the stress function over that cell. As ever, reciprocal points are then connected by lines, there being a line between points if the two cells share a face.

We illustrate the construction for the window-frame-on-supports example of Fig. 18, shown again here in Fig. 19. Fig. 19a shows the structure and Fig. 19b shows how the full space around the structure is partitioned into cells, with the stress function linear across each cell, but possibly discontinuous across cell boundaries. As discussed previously, and as in standard 2D graphic statics using an Airy stress function, the cells external to the structure may equally be considered to be internal. This representation is shown in Fig. 19c. This has the same connectivity, the only difference being that cells 2 and 4 may now be identified as being the same cell. There are thus 8 cells, and hence the reciprocal diagram has 8 nodes . In this case the Rankine reciprocal - shown in Fig. 19d) - is planar, consisting of a set of overlapping rectangles.

In a standard Rankine reciprocal, each bar has a reciprocal polygon perpendicular to the bar, the area of the polygon representing the axial force in the bar. This can be seen in the window frame example here, since the lines of the reactions through the supports are purely axial, and carry a force gh. Inspection of Fig. 19b shows the line of the upper left reaction to be a shared edge of the cells 1, 5, 6 and 2, and there is a rectangle 1562 of area gh within the reciprocal diagram, and

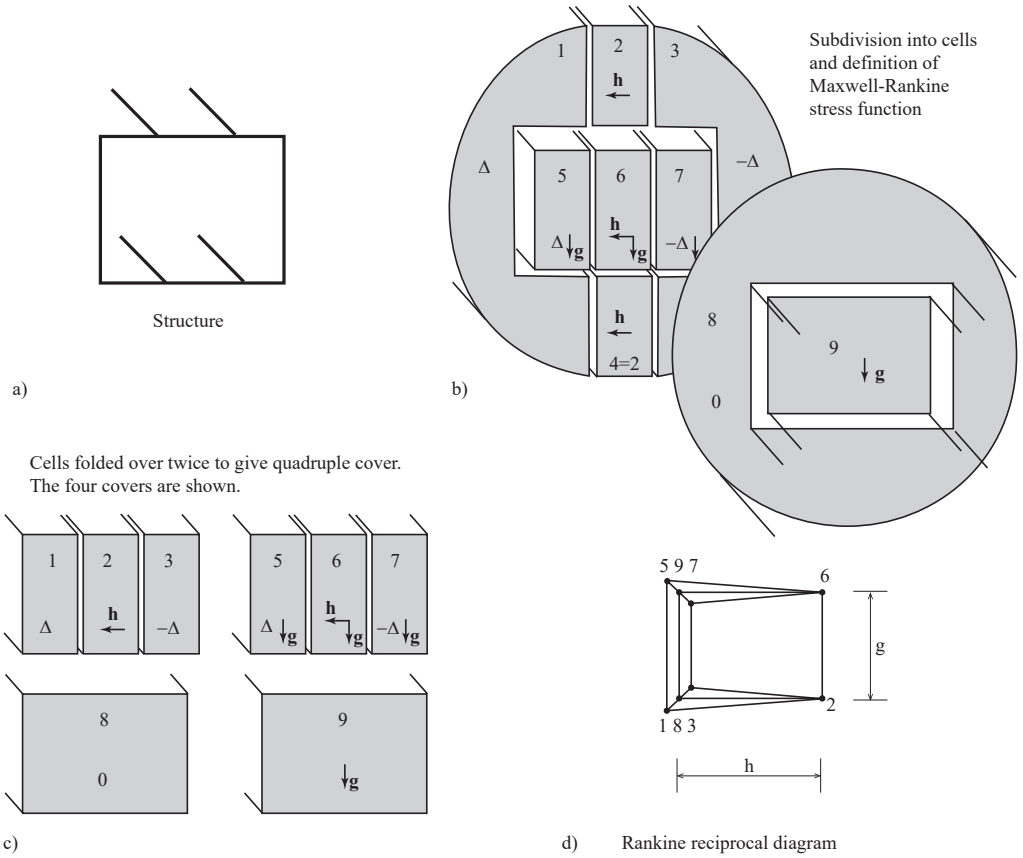

Figure 19: a) The window frame structure on supports of Fig. 18. b) The subdivision of the surrounding space into cells over each of which the Maxwell-Rankine stress function is linear. c) An alternative representation of the cell subdivision, where cells previously external to the structure are considered to be internal. The result is a quadruple cover of the rectangular prism that extends to one side of the structure. This representation leads to a reduced cell count, since cells 2 and 4 may now be identified. There are thus 8 distinct cells. d) The Rankine reciprocal obtained by plotting nodes at the negative of the gradients over the eight original cells. The stress function over cells 1,3 and 8 have no gradient, such that their reciprocal nodes, although topologically distinct, all lie at the reciprocal origin. Reciprocal nodes 5,7 and 9 are likewise distinct but coincident at the point $(0, -g, 0)$. Coincident nodes have been drawn separated for clarity.

which is perpendicular to the line through the support.

The meaning of the other rectangles in the reciprocal will now be determined. These are illustrated in Fig. 20. Upper left shows the axial force in bar 1562 as a reciprocal rectangle of area gh perpendicular to the bar.

Lower left shows the reciprocal for the grillage beam running around the left side of the structure. This beam is the common edge of cells 1,5,9 and 8, and its reciprocal is a rectangle of zero area, but of height g. For the cross-beam part (which is in pure bending) the thin reciprocal rectangle is perpendicular to that part of the beam. For the edge beam which is in torsion, the thin reciprocal rectangle is parallel to the beam. These alignments accord with those that arose

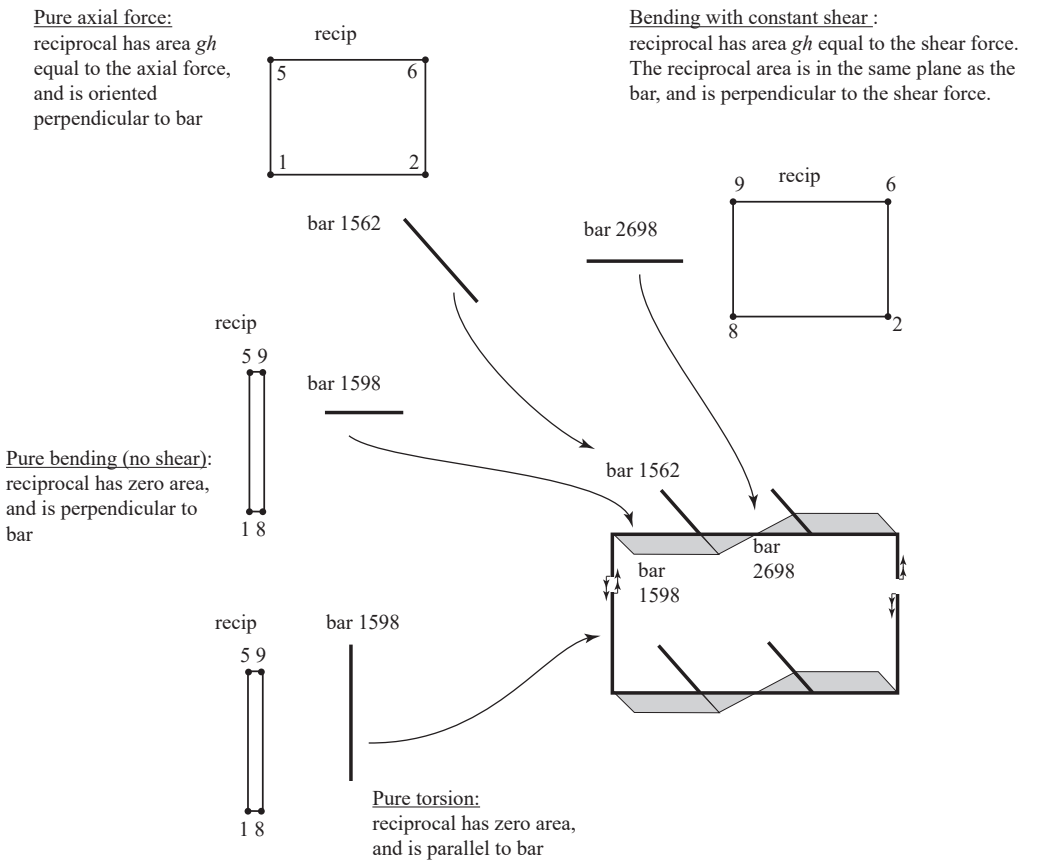

Figure 20: The meaning of the various components of the Rankine reciprocal for the window-frame-on-supports example. Upper left shows the standard Rankine reciprocal for a bar carrying a purely axial load, such as the support line 1562, where the axial force is given by the area gh of the reciprocal rectangle perpendicular to the bar. The polygons reciprocal to three other bars are shown.

in 2D graphic grillage analysis, although the magnitude $g\Delta$ of the moment is no longer available graphically, but must be determined by reference back to the discontinuity Δ in the original stress function. This is akin to the situation in the Williams and McRobie [1] description of moments in 2D frames. There, forces are given by lengths in the Maxwell reciprocal but the moments are found in the discontinuities in the Airy stress function over the *original* diagram.

The most interesting feature of the reciprocal diagram concerns the crossbeam section between supports, over which the bending moment varies linearly. This segment of the beam is the common edge of cells 2,6,9 and 8 and there is a reciprocal rectangle 2698 of area gh within the Rankine reciprocal diagram. This rectangle is not perpendicular to the original member, but rather the rectangle and the beam are co-planar, with the rectangle perpendicular to the direction of the shear force. The rectangle has area gh, this being the magnitude of the shear force. This is a new manifestation of the Rankine reciprocal, where the area of the reciprocal polygon, rather than being an axial force, is the shear force in the beam.

Given an original and a reciprocal, it is possible to construct a grillage-Minkowski diagram which combines the two. This is illustrated in Fig. 21. Although the resulting diagram is somewhat complicated, it demonstrates that showing that the machinery that has been developed in recent papers for handling 2D and 3D trusses carries over to the 3D grillage case. Moreover, since the reciprocal is planar and in the plane of the window-frame, it gives a clear demonstration of the point that Rankine reciprocal polygons need no longer be orthogonal to their original members. Whether further load path theorems then follow from such a construction is left for further research.

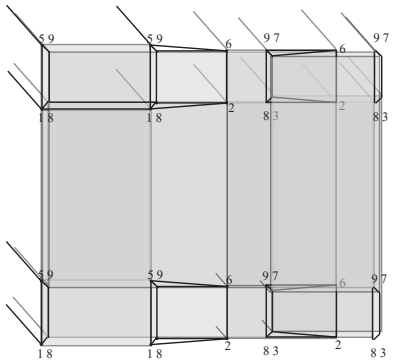

Figure 21: The grillage-Minkowski diagram for the window-frame-on-supports. Coincident nodes have been separated for clarity.

10 A grillage beam carrying torsion, bending and shear

Thus far we have shown how a stress function approach can be constructed for grillages where members in torsion interact with members in bending and shear. Here, we show how to represent a single beam which exhibits all three effects.

Fig. 22a shows a vertical cantilever, like a flagpole, which carries a lateral tip load. At a distance L below the tip, an external torsional couple is applied, such that the lower part of the pole is in combined torsion, bending and shear.

Fig. 22b shows the Maxwell-Rankine stress function. For $x > L$, the function is

$$\Phi(x, y, z) = kxH(y) + g(x - L)K(z) + hq(z) \tag{25}$$

where $H(y)$ and $K(z)$ are appropriate smooth unit step functions, and $q(z)$ is a smoothed unit slope discontinuity (such as $q = z^2/2D$, where D is the (vanishingly) small bar thickness in the z direction).

The matrix of second derivatives is

$$\Phi_{,ij} \quad = \quad \begin{pmatrix} 0 & kH_{,y} & gK_{,z} \\ kH_{,y} & kxH_{,yy} & 0 \\ gK_{,z} & 0 & g(x-L)K_{,zz} + hq_{,zz} \end{pmatrix} \tag{26}$$

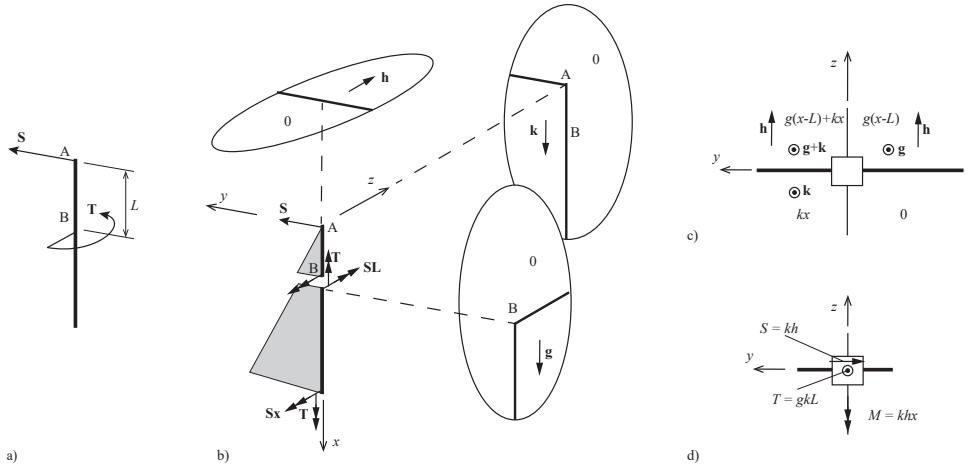

Figure 22: a) A cantilever subject to a lateral tip load $\boldsymbol{S}$ and an external couple $\boldsymbol{T}$ applied a distance L below the tip. b) The Maxwell-Rankine stress function. c) The stress function morphology on a cross-section perpendicular to the lower part of the cantilever. d) The resulting stress resultants.

whose co-factors give the stresses on the plane as

$$\sigma_{xx} = kxH_{,yy}\left(g(x-L)K_{,zz} + hq_{,zz}\right) \tag{27}$$

$$\sigma_{xy} = -kH_{,y}\left(g(x-L)K_{,zz} + hq_{,zz}\right) \tag{28}$$

$$\sigma_{xz} = -kxH_{,yy}\left(gK_{,z}\right) \tag{29}$$

$$\tag{30}$$

Integrating the stresses over the (vanishingly small) rectangular bar area of $0 < y < B$ by $0 < z < D$, we use the identity $\int H_{,yy}\ dy = [H_{,y}] = 0$ (since the step function slope is zero at either edge of the bar) to obtain $P_{xx} = 0$ and $S_{xz} = 0$. There is however non-zero shear force S_{xy}. We use $\int H_{,y}\ dy = [H] = 1$, together with $\int K_{,zz}\ dz = 0$ and $\int q_{,zz}\ dz = [q_{,z}] = 1$ to obtain $S_{xy} = -kh$.

Looking along the applied tip load, we see a Mairy stress function involving only the orthogonal gradient changes k and h, with no step discontinuities. The reciprocal diagram is thus a rectangle of side lengths k by h, thus the applied tip load $\boldsymbol{S}$ is of magnitude kh. This is equal to the shear S_{xy} in the cantilever, as just calculated.

For the bending moments, we have $M_{yy} = \int z\sigma_{xx}\ dy\ dz$ and again the identity $\int H_{,yy}\ dy = 0$ shows that M_{yy} is zero.

For $M_{zz} = \int y\sigma_{xx}\ dz$ we use $\int yH_{,yy}\ dy = [yH_{,y}] - \int H_{,y}\ dy = 0 - [H] = -1$. For the z integration, we have $K_{,zz}$ and $q_{,zz}$ integrating to zero and unity respectively. Together, these give $M_{zz} = -khx$. This is the linearly-varying bending moment due to the tip load kh. Thus far, the analysis is consistent with, and indeed almost identical to, our earlier analysis for a beam carrying shear and bending, in that the torsional terms (due to the stress function part involving the gradient $\boldsymbol{g}$) have all dropped from the analysis. We now consider the torsional part.

For this, we require

$$T_{xx} = \int\ z\sigma_{xy} - y\sigma_{xz}\ dy\ dz \tag{31}$$

For the first term, we use the identities $\int H_{,y}\ dy = 1$ and $\int zK_{,zz}\ dz = -1$, together with

$\int zq_{,zz}\ dz = D/2$ (this latter going to zero in the limit of vanishing bar thickness). These give $\int z\sigma_{xy}\ dy\ dz = kg(x - L)$.

For the second term, we use $\int yH_{,yy}\ dy = -1$ and $\int K_{,z}\ dz = 1$ to obtain $\int y\sigma_{xz}\ dy\ dz = kgx$. Combining the two we obtain

$$T_{xx} = kg(x - L) - kgx = -gkL \tag{32}$$

Remarkably, the x variations cancel, leaving a constant torsion of magnitude gkL. This can be written $g\Delta$, where $\Delta = kL$ is the magnitude of the discontinuity at the point where the couple is applied. This then matches our earlier derivation for the pure torsion case.

We have thus arrived at a 3D Maxwell-Rankine stress function description for a beam carrying combined torsion, bending and shear. Such elements can now be combined to build more complex 3D structures. For example, the couple $\boldsymbol{T}$ applied part way down the cantilever may be applied via the end moment of a horizontal beam in bending, the beam connecting in at a right-angle, as in the earlier example of the window-frame-on-supports. We leave the creation of such examples as a topic for further research and development. Although there were numerous integrals involved in the derivations here, it is envisaged that more complex structures can now be analysed by simply combining the elementary stress function morphologies.

We also note that additional stress function features can readily be incorporated. For example, the y, z variation could have two orthogonal slope changes, $\boldsymbol{h}$ and $\boldsymbol{j}$ say. This would generate and axial force hj along the x-axis. However, as in the earlier example of biaxial bending, the various stress function components then begin to interact. The inclusion of an axial force in this manner would also generate a shear force $S_{xz} = -jg$. As per the biaxial case, further subdivision of the surrounding cells would allow more freedom, but at the expense of increased complexity. We leave for future the development of methods that best accomplish such generalisations in the simplest manner.

11 Summary and Conclusions

This paper has taken some steps towards creating a graphic statics for 3D frames. It is a 3D generalisation of the Williams and McRobie [1] approach to 2D frame analysis, which used discontinuous Airy stress functions. For 3D frames, the fundamental object is a discontinuous Maxwell-Rankine stress function, as described in Section 2. Sections 3-5 developed the stress functions for isolated beams in space, these being capable of exhibiting biaxial bending or torsion. Section 6 looked at the first of two special cases of the fully 3D theory: this was a demonstration of consistency, showing how the 2D Williams-McRobie theory could be extracted from the 3D theory. More interestingly, Section 7 showed another special case which revealed a new 2D theory - for the graphic analysis of plane grillages with no shear. This theory shared many similarities with the theory for 2D trusses, but was more general in that lines need no longer be perpendicular to their reciprocals. A number of simple examples were given. Other ideas from 2D truss analysis were then derived for the 2D grillage theory, including the notions of grillage-Minkowski diagrams and analogous Load Path Theorems. Section 8 took the first steps towards coupling together the various actions in 3D for the representation of a simple space beam. Section 9 looked at how to incorporate beams with shear and bending into the grillage analysis. One interesting result was how the Rankine reciprocal was a polygon oriented in the direction of the shear force, rather than orthogonal to the beam. Finally Section 10 showed a stress function representation for a beam carrying combined torsion, bending and shear. In summary, these developments describe the foundations for a conceptual framework which it is hoped can subsequently be applied in the design of real 3D structures.

References

[1] Williams C. J. K and McRobie A. Graphic statics using discontinuous Airy stress functions. *International Journal of Space Structures*, 2016.

[2] McRobie A. Rankine reciprocals with Zero Bars. *International Journal of Solids and Structures*, Submitted, 2016.

[3] Maxwell J.C. On reciprocal figures and diagram of forces. *Philos. Mag.*, 26:250–261, 1864.

[4] Maxwell J.C. On reciprocal figures, frames and diagrams of forces. *Trans. Roy. Soc. Edinburgh*, 7:160–208, 1870.

[5] Rankine W.J.M. *A Manual of Applied Mechanics*. C. Griffin and Co., London, 1858.

[6] Mitchell T., Baker W., McRobie A., and Mazurek A. Mechanisms and states of self-stress of planar trusses using graphic statics, Part I. *International Journal of Space Structures*, 2016.

[7] McRobie A., Baker W., Mitchell T., and Konstantatou M. Mechanisms and states of self-stress of planar trusses using graphic statics, Part II. *International Journal of Space Structures*, 2016.

[8] McRobie A. Maxwell and Rankine reciprocal diagrams via Minkowski sums for 2D and 3D trusses under load. *International Journal of Space Structures*, 2016.

[9] Akbarzadeh M., Van Mele T., and Block P. Equilibrium of spatial structures using 3-D reciprocal diagrams. *Proc. IASS , Wroclaw*, 63, 2013.

[10] Akbarzadeh M., Van Mele T., and Block P. On the equilibrium of funicular polyhedral frames and convex polyhedral force diagrams. *Computer-Aided Design*, 63:118–128, 2015.

[11] M. Akbarzadeh, T. Van Mele, and P. Block. 3d graphic statics: Geometric construction of global equilibrium. In *Proceedings of the International Association for Shell and Spatial Structures (IASS) Symposium*, Amsterdam, August 2015.

[12] Micheletti A. On generalized reciprocal diagrams for self-stressed networks. *International Journal of Space Structures*, 23(3):153–166, 2008.

[13] Beghini L.L., Carrion J., Beghini A., Mazurek A., and Baker W.F. Structural optimization using graphic statics. *Struct. Multidisc. Optim.*, 2013.